Original Article

MOLECULAR METABOLISM

Dynamics of vitamin A uptake, storage, and utilization in vocal fold mucosa

Kohei Nishimoto [1,3], Yutaka Toya [1,4], Christopher R. Davis [2], Sherry A. Tanumihardjo [2], Nathan V. Welham [1,*]

ABSTRACT

Objective: Extrahepatic vitamin A is housed within organ-specific stellate cells that support local tissue function. These cells have been reported in the vocal fold mucosa (VFM) of the larynx; however, it is unknown how vitamin A reaches and is disseminated among VFM target cells, how VFM storage and utilization vary as a function of total body stores, and how these parameters change in the context of pathology. Therefore, in this study, we investigated fundamental VFM vitamin A uptake and metabolism.

Methods: Using cadaveric tissue and serum from human donors representing the full continuum of clinical vitamin A status, we established a concentration range and analyzed the impact of biologic and clinical covariates on VFM vitamin A. We additionally conducted immunodetection of vitamin A-associated markers and pharmacokinetic profiling of orally dosed α-retinyl ester (a chylomicron tracer) in rats.

Results: Serum vitamin A was a significant predictor of human VFM concentrations, suggesting that VFM stores may be rapidly metabolized *in situ* and replenished from the circulatory pool. On a vitamin A-sufficient background, dosed α-vitamin A was detected in rat VFM in both ester and alcohol forms, showing that, in addition to plasma retinol and local stellate cell stores, VFM can access and process postprandial retinyl esters from circulating chylomicra. Both α forms were rapidly depleted, confirming the high metabolic demand for vitamin A within VFM.

Conclusion: This thorough physiological analysis validates VFM as an extrahepatic vitamin A repository and characterizes its unique uptake, storage, and utilization phenotype.

Keywords α-retinol; Retinol; Extrahepatic stellate cell; Human cadaver; Larynx; Macula flava; Rat model

1. INTRODUCTION

Vitamin A is an essential dietary molecule. It underpins vision (as the retinal chromophore) and is critical for an array of cellular functions, including proliferation, differentiation, and morphogenesis [1,2]. Most vitamin A is stored as retinyl esters in hepatic stellate cells and released to the circulatory pool as retinol-binding protein 4 (RBP4)-bound retinol for transport to extrahepatic tissues [3,4]. Alternatively, retinyl esters can be transported to extrahepatic sites postprandially by RBP4-independent chylomicra [5,6]. The relative contribution of RBP4- and chylomicron-mediated transport to extrahepatic target cells varies as a function of the target organ and total body vitamin A status [5,7–9].

Outside of the liver, vitamin A stores have been identified in the stellate cells of various extrahepatic tissues, such as the pancreas, kidneys, spleen, lungs, and larynx [3,4]. These local tissue repositories provide a readily available source of vitamin A to resident cells with high metabolic needs. In the vocal fold mucosa (VFM) of the larynx, VF stellate cells housed within discrete anatomic niches called the macula flavae (MF) store vitamin A [10,11], whereas nearby VF epithelial cells have no known storage capacity but are highly responsive to vitamin A bioavailability [12–14]. Vitamin A deficiency leads to local depletion from VF stellate cells [12], epithelial hyperkeratosis [13], and if the deficiency occurs during embryogenesis, profound laryngotracheal malformation [14].

Despite the evidence of vitamin A's importance to VF stellate and epithelial cell biology and its relevance to clinical disorders [15], there are no physiological studies of vitamin A uptake and utilization within the larynx. Such data are needed to better understand how vitamin A reaches VFM target cells, how VFM storage and utilization vary as a function of total body vitamin A stores, and how these parameters change in the context of pathology. In this study, we addressed these knowledge gaps using cadaveric tissue and serum from human donors representing the full continuum of clinical vitamin A status (deficient through hypervitaminotic), vitamin A-sufficient and -deficient *in vivo* rat models, and pharmacokinetic profiling of the α form of vitamin A, which cannot bind RBP4. We established a vitamin A concentration range for VFM; explored the impact of biologic and clinical covariates on VFM storage; compared vitamin A-specific uptake, processing, and utilization markers across VF cell subpopulations; and tested the capacity of VFM to uptake postprandial vitamin A directly from chylomicra. This cross-species phenotypic characterization provides a

[1]Division of Otolaryngology, Department of Surgery, University of Wisconsin School of Medicine and Public Health, Madison, WI, 53792, USA [2]Department of Nutritional Sciences, University of Wisconsin-Madison, Madison, WI, 53706, USA

[3] Currently affiliated with the Department of Otolaryngology, Kumamoto University, Kumamoto 860-8556, Japan.
[4] Currently affiliated with Isshiki Memorial Voice Center, Kyoto ENT Surgicenter, Hiroshiba ENT Clinic, Kyoto 610-0355, Japan.

*Corresponding author. K4/723 CSC, 600 Highland Avenue, Madison, WI, 53792, USA. E-mail: welham@surgery.wisc.edu (N.V. Welham).

Received March 16, 2020 • Revision received May 11, 2020 • Accepted May 23, 2020 • Available online 28 May 2020

https://doi.org/10.1016/j.molmet.2020.101025

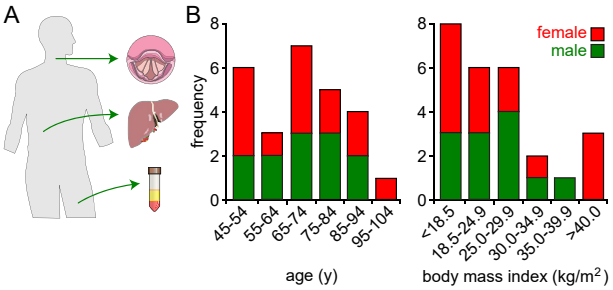

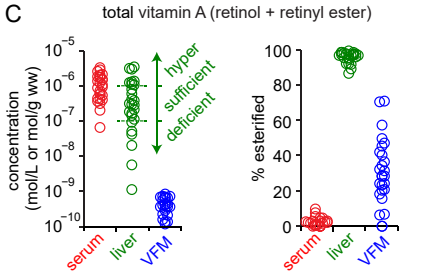

D ANCOVA
Dependent variable: total vitamin A concentration in VFM

Source	df	R^2	F	P
model	5	0.6182	6.48	0.0010
error	20			
total	25			
Main effects				
age	1		2.94	0.1021
sex	1		0.22	0.6462
body mass index	1		0.01	0.9067
serum concentration	1		6.83	0.0008
liver concentration	1		15.56	0.0166

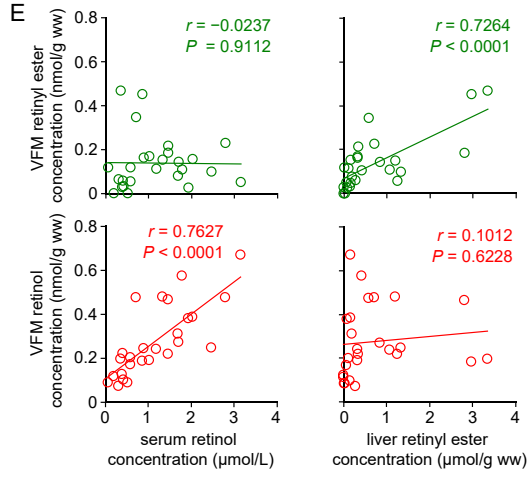

Figure 1: Vitamin A storage profiles in human VFM compared to liver and serum. (A) Schematic of human biospecimen procurement. Bilateral VFM, liver biopsies, and sera were harvested from 26 adult cadavers <16 h postmortem. (B) Age, sex, and body mass index distributions in the cadaver cohort. (C) Total vitamin A concentrations and percent esterified vitamin A in human serum, liver, and VFM. Green dashed lines indicate liver-based cutoffs for vitamin A deficiency ($n = 6$) and hypervitaminosis A ($n = 8$). (D) ANCOVA output summarizing the associations between the concentration of total vitamin A in VFM and that of serum and liver as well as age, sex, and body mass index. (E) Scatterplots and Pearson's r statistics showing the associations between the concentrations of VFM retinyl ester and serum retinol, VFM and liver retinyl ester, VFM and serum retinol, and VFM retinol and liver retinyl ester.

foundation for future research into vitamin A biology and clinical disorders of the larynx.

2. MATERIALS AND METHODS

2.1. Human tissue procurement

Human biospecimens were obtained with approval of the University of Wisconsin Health Sciences Institutional Review Board; specimens intended for vitamin A analyses were procured by the National Disease Research Interchange. Whole larynges, liver biopsies (5 × 5 × 10 cm), and blood sera (5 mL, isolated from whole blood via gel separation and centrifugation) were harvested from 26 cadavers (12 males, 14 females, age 49–101 y; Figure 1B) < 16 h postmortem. Two donors (1 male and 1 female) were identified as Hispanic or Latino, White; 24 donors (11 males and 13 females) were identified as non-Hispanic or Latino, White. Samples were snap-frozen in liquid N_2, transported to our laboratory on dry ice, and stored at -80 °C until use. An additional 8 human larynges were procured from autopsy cadavers (6 males, 2 females, age 40–68 y) < 36 h postmortem and processed for immunoblotting ($n = 5$) and histology and immunohistochemistry ($n = 3$).

The donors had no history of chemoradiation to the head and neck region, had not undergone prolonged endotracheal intubation or ventilation prior to death, were not septic, and had negative infectious disease serology. All of the donors had a negative history for laryngeal disease; all of the larynges were considered normal at autopsy and during tissue microdissection. One donor had a positive history of liver cirrhosis. The causes of death were cardiopulmonary events in most cases, esophageal cancer sequelae in one case, granulomatosis with polyangiitis sequelae (but no laryngeal involvement) in one case, dementia sequalae in one case, and unknown in two cases.

Liver and serum data from this cohort were included in a previously reported analysis of the relationship between serum retinyl esters and total liver vitamin A reserves [16]; this prior analysis included one additional cadaver from whom we procured liver and serum but no larynx.

2.2. Compound synthesis

α-Retinyl acetate was synthesized using a previously described method for synthesizing ^{13}C-retinyl acetate [17] with the following modifications: α-ionone (Sigma Aldrich) was used in place of β-ionone as the starting reagent and ^{13}C was not added. The synthesized α-retinyl acetate was purified (>95%) on 8% water-deactivated neutral Al_2O_3 using hexanes and diethyl ether; purity was confirmed by thin-layer chromatography, ultraviolet (UV)-visible spectroscopy, and high-performance liquid chromatography (HPLC) with photodiode array detection.

2.3. Animals, diet, and compound dosing

Animal experiments were conducted in accordance with the Public Health Service Policy on Humane Care and Use of Laboratory Animals and the Animal Welfare Act (7 U.S.C. et seq.); the protocols were approved by the University of Wisconsin School of Medicine and Public Health Animal Care and Use Committee. We used a rat model as rats have documented vitamin A-storing stellate cells in the anterior and posterior MF (aMF and pMF, respectively) [11] and tolerate oral dosing of α-retinyl acetate [18].

The rats were housed in a temperature- and humidity-controlled environment with a 12-h light–dark cycle. Aspen bedding was used as it absorbs moisture, eliminates odor, and has low nutritional value (maize cobs, another option, would have interfered with our bioassays

due to kernel contamination). The rats were placed on a vitamin A-free purified diet *ad libitum* to attenuate their preexisting hyper-supplemented status and obtain the intended vitamin A sufficiency or deficiency targets. The vitamin A-deficient diet (TD.04175; Harlan-Teklad) contained the following (in g/kg): casein (200); DL-methionine (3); sucrose (280); maize starch (215); maltodextrin (150); cellulose (50); soybean oil (55); mineral mix AIN-93G (TD.94046) (35); calcium phosphate (3.2); vitamin mix without added A, D, E, and choline (TD.83171) (5); vitamin D_3 (0.0044); vitamin E (0.242); choline dihydrogen citrate (3.5); and *tert*-butylhydroquinone (0.01).

In our preliminary experiment, 3-week-old male weanling Sprague Dawley rats ($n = 75$; Charles River) were vitamin A-depleted for 3 weeks to obtain vitamin A deficiency. Next, the rats received a single 1 mg (3.5 μmol) oral dose of α-retinyl acetate in cottonseed oil vehicle ($n = 70$); the control rats ($n = 5$) received no dose. The rats were euthanized at 0 (control), 0.5, 1, 1.5, 2, 3, 4, 6, 8, 12, 24, 48, 96, 168, and 336 h post-dose; blood, liver, and kidneys were collected at each time point. Tissue wet weights were recorded.

In our primary experiment, 5-week-old male Fischer 344 rats ($n = 65$; Charles River) were vitamin A-depleted for 3 weeks to obtain a marginal vitamin A status. Next, the rats received a single 2 mg (7 μmol) oral dose of α-retinyl acetate in cottonseed oil vehicle ($n = 55$); the control rats were dosed with vehicle only ($n = 5$) or received no dose ($n = 5$). Approximately 250 μL of blood was collected from the saphenous vein of 5–6 α-retinyl acetate-dosed rats per time point at 0 (no dose control), 1, 3, 5, 9, 11, and 24 h post-dose. We sampled different animals at each time point as serial blood draws would have caused unacceptable blood volume loss. The rats were euthanized at 7 ($n = 30$) or 72 h ($n = 25$) post-dose; the vehicle control rats were euthanized at 7 h post-dose. Blood, larynx, liver, lungs, kidneys, and spleen were collected at each time point. Tissue wet weights were recorded.

2.4. Serum processing for liquid chromatography

2.4.1. Human

Human serum samples were processed as 500 μL aliquots; 1.25 × volume of ethanol was added to denature proteins. The internal standard C-23 β-*apo*-carotenol was added to determine extraction efficiencies. Samples were extracted three times with 0.75 mL hexanes; supernatant fractions were pooled, dried under N_2, and reconstituted in 100 μL methanol:dichloroethane (75:25, v/v). Two μL was injected into the ultra-performance liquid chromatography (UPLC) instrument.

2.4.2. Rat

Rat serum samples were processed as previously described for human serum with the following modifications. In the preliminary experiment, extractions were reconstituted in 100 μL methanol:dichloroethane (50:50, v/v) and 50 μL was injected into the HPLC instrument. In the primary experiment, the starting volume of serum from all of the saphenous vein draws was 35–100 μL, extractions were reconstituted in 30 μL methanol:dichloroethane (75:25, v/v), and 2 μL was injected into the UPLC instrument.

2.5. Tissue processing for liquid chromatography

2.5.1. Human

Human larynges and liver samples were transferred to room temperature (RT) for 60 min and then dissected. Bilateral VFM were microdissected from each larynx with retention of both aMF and pMF and then weighed. Each liver sample was dissected and weighed to obtain a 1 g sample for vitamin A analyses; surplus tissue was retained for protein isolation and immunoblotting.

Bilateral VFM pairs were immersed in 1 mL of ethanol and 20 μL of C-23 β-*apo*-carotenol was added. The tissue was minced with scissors, 500 μL of phosphate-buffered saline (PBS) was added, and the entire solution was homogenized (Tissue-Tearor 985370; Biospec). Each sample was transferred to a glass tube and the homogenization tube was rinsed twice with 1 mL of ethanol and once with 2 mL of hexanes; each rinse solution was added to the sample tube followed by an additional 1 mL of PBS. The non-polar hexane layer was then transferred to a new tube and the extraction was repeated twice, each time using 2 mL of hexanes. Finally, all of the extraction fractions were pooled, dried under N_2, and reconstituted in 20 μL methanol:dichloroethane (50:50, v/v). Four μL was injected into the UPLC instrument.

Human liver tissue (1 g) was ground with 4–5 g of sodium sulfate in a mortar and pestle; 500 μL of C-23 β-*apo*-carotenol was added. The samples were extracted repeatedly with dichloromethane through a Whatman #1 filter (GE Healthcare) to a 50 mL volume. A 5 mL aliquot was dried under N_2 and reconstituted in 300 μL methanol:dichloroethane (75:25, v/v). One μL was injected into the UPLC instrument.

2.5.2. Rat

Rat larynges were microdissected and each VFM (with retention of both aMF and pMF) was removed and then weighed. Prior studies demonstrated that the accurate quantification of vitamin A in rat VFM requires pooling across animals [11]; based on pilot UPLC data, we pooled bilateral VFM from sets of 5 larynges per biological replicate. Pooled rat VFM samples were processed as previously described for human VFM with the following modifications: the initial ethanol volume was 500 μL and post-homogenization rinses were performed twice with 500 μL ethanol and once with 1 mL hexanes.

Rat liver (0.5 g), lung (whole), kidney (1 g), and spleen (whole) samples were processed as previously described for human liver with the following modifications. Liver, lung, and spleen samples were extracted to a 50 mL final volume and kidney samples were extracted to a 25 mL final volume. For the liver and kidney samples, a 5 mL aliquot was dried under N_2; for the lung and spleen, the entire sample was dried with a rotary evaporator (Rotavapor R-114; Buchi) coupled with a circulation chiller (WK230; Lauda-Brinkman), re-dissolved three times in 1 mL of dichloromethane, and then dried under N_2. The extractions were reconstituted in 100 μL (lung), 200 μL (liver), or 250 μL (kidney and spleen) of methanol:dichloroethane (75:25, v/v). In the preliminary experiment, 50 μL of liver or 25 μL of kidney reconstituted extract was injected into the HPLC instrument; in the primary experiment, 2 μL (all of the tissues) was injected into the UPLC instrument.

2.6. Liquid chromatography

The rat preliminary experimental samples were analyzed as follows. The serum was analyzed using an isocratic HPLC system comprising a guard column, a Waters Symmetry C18 column (3.5 μm, 4.6 × 75 mm), a Waters Resolve C18 column (5 μm, 3.9 × 300 mm), a Rheodyne injector, a Shimadzu SPD-10A UV-visible spectroscopy detector, a Waters Delta 600 pump and controller, and a Shimadzu C-R7A Plus data processor. Tissue was analyzed using the columns and a Waters 1525 binary HPLC pump, a Waters 717 autosampler, and a Waters 996 photodiode array detector. The mobile phase was acetonitrile:water (87.5:12.5, v/v); 10 mmol of ammonium acetate was used as a modifier, and the flow rate was 0.7 mL/min.

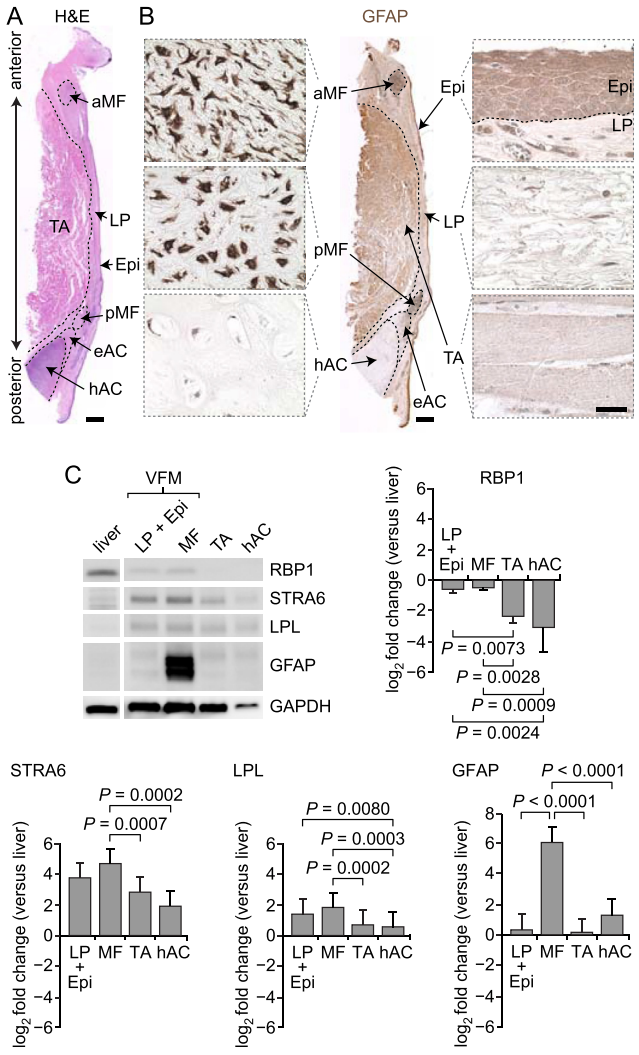

Figure 2: Characterization of stellate cell- and vitamin A-associated markers in human VF. (A) Representative H&E-stained axial section of the human VF procured from a 69-y-old male donor. The black dashed lines indicate the anterior and posterior macula flavae (aMF and pMF), hyaline and elastic regions of the arytenoid cartilage (hAC and eAC), and the boundary between the thyroarytenoid muscle (TA) and lamina propria (LP). Epi, epithelium. Scale bar, 1 mm. (B) Adjacent axial section immunostained for GFAP. Scale bar, 1 mm (low-magnification image); 50 μm (high-magnification images). (C) Representative Western blotting and densitometric analysis showing the relative abundance of RBP1, STRA6, LPL, GFAP, and GAPDH in human LP + Epi, MF, TA, and hAC compared to the liver. The variation in GAPDH abundance across conditions (despite a consistent 10 μg protein load) reflects differences in tissue cellularity. Data are shown as means ± SEM; *P* values were calculated using a one-way ANOVA ($n = 5$ per condition); unannotated pairwise comparisons indicate non-significant differences.

All of the human cadaver and rat primary experimental samples were analyzed using a Waters Acquity UPLC HSS C18 1.8-μm VanGuard pre-column in conjunction with a Waters Acquity UPLC HSS C18 column (1.8 μm, 2.1 × 150 mm). The method utilized two solvent mixes run in a 29-min gradient: solvent A was acetonitrile:water:propanol (70:25:5, v/v/v) with 10 mmol ammonium acetate; solvent B was methanol:propanol (75:25, v/v). The gradient began with 100% solvent A for 7 min, a linear transition to 5% solvent A over 4 min, a further transition to 1% solvent A over 12 min, a reversal to 100% solvent A over 2 min, and maintenance of 100% solvent A for the final 4 min. The column temperature was 32 °C, and the flow rate was 0.4 mL/min.

HPLC and UPLC detection was set at 311 nm for α-retinol and α-retinyl ester and 325 nm for retinol and retinyl ester (Figure 3B shows representative spectra; Figures 3D, 4B, and S2A show representative chromatograms). Retinyl oleate and palmitate coeluted in this system (as did α-retinyl oleate and palmitate). Concentrations were calculated using curves generated via analysis of HPLC-purified standards.

2.7. Histology and immunohistochemistry

Human larynges ($n = 3$) were microdissected and each VF (VFM including aMF and pMF, elastic and hyaline regions of the arytenoid cartilage [eAC and hAC, respectively], and thyroarytenoid muscle [TA]) was removed *en bloc*. Tissue was fixed in 4% paraformaldehyde for 24 h, dehydrated in 70% ethanol, and 5-μm-thick paraffin sections were prepared. Sections intended for morphological assessment were stained with hematoxylin and eosin (H&E). Sections intended for immunostaining were processed for antigen retrieval in a decloaking chamber (BioCare Medical) using 10 mM of citrate buffer (pH 6.0), permeabilized using 0.2% Triton X-100 for 10 min, blocked with 10% bovine serum albumin in PBS for 60 min, and incubated with primary antibodies at 4 °C overnight. For horseradish peroxidase (HRP)-based detection, endogenous peroxidase was quenched using 3% H_2O_2 in PBS. ImmPRESS anti-mouse and anti-rabbit immunoglobulin G (IgG) HRP polymers were used for secondary detection (30 min incubation time) and an ImmPACT DAB kit was used to develop the signal according to the manufacturer's instructions (all of the reagents were obtained from Vector Labs). Sections were counterstained with hematoxylin, dehydrated, cleared, and cover-slipped.

Rat larynges and livers ($n = 3$ per organ) were harvested *en bloc*, dehydrated in 20% sucrose, embedded in optimal cutting temperature compound (Tissue-Tek, Sakura Finetek), and snap-frozen in liquid N_2. Five-μm-thick cryosections were prepared (for larynges, in the axial plane; for livers, in any orientation), fixed using either 4% paraformaldehyde at RT, methanol at 4 °C, or acetone at -20°C, and air dried at RT. The sections were washed with PBS and blocked with 5% goat serum and 0.02% Tween 20 in PBS at RT for 30 min. The sections were sequentially incubated with primary antibodies at 4 °C overnight, relevant secondary antibodies (Alexa Fluor 488- or 594-conjugated, goat anti-mouse, and goat anti-rabbit IgG [1:400; A-11001, A-11008, A-11005, and A-11012, Invitrogen]) at RT for 1 h, and nuclear dye DAPI (1 μg/mL; Sigma—Aldrich) at RT for 5 min. A subset of slides were additionally incubated with lipophilic dye BODIPY 505/515 (5 μM; D-3921, Thermo Fisher) prior to DAPI. The slides were covered with antifade mounting medium (Sigma—Aldrich) and cover-slipped.

Imaging was performed using a Nikon Ti-S/L100 inverted microscope connected to DS-Qi2 (Nikon) and Infinity 1-1 (Lumenera) digital cameras; images were captured with consistent exposure settings. Negative control sections stained without either the primary or secondary antibody showed no immunoreactivity. The primary antibodies used were: mouse anti-GFAP (1:200 [human], 1:100 [rat]; G3893, Sigma—Aldrich); rabbit anti-GFAP (1:100 [rat]; RB-087-A1, Thermo Fisher); rabbit anti-STRA6 (1:1000 [human], 1:100 [rat]; bs-12351 R, Bioss); rabbit anti-LPL (1:200 [human]; sc-32885, Santa Cruz); mouse anti-LPL (1:50 [rat]; MABS1350, EMD Millipore); rabbit anti-RBP1 (1:100 [human]; sc-30106, Santa Cruz); mouse anti-RARA (1:200 [human and rat]; MAB5346, EMD Millipore); mouse anti-PLIN1 (undiluted hybridoma supernatant [rat]; 651156, Progen).

2.8. Immunoblotting

Human larynges ($n = 5$) were microdissected and the following VF subsites were harvested and processed separately: mid-membranous lamina propria and epithelium (LP + Epi, not including MF); aMF and

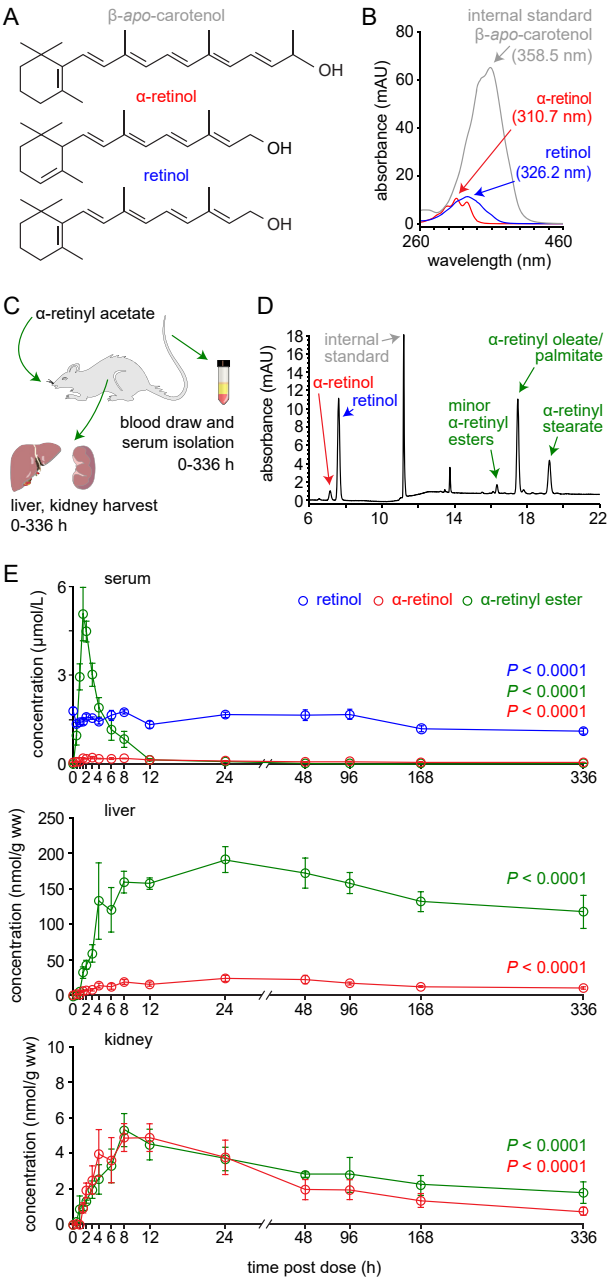

Figure 3: Pharmacokinetics of single dose α-retinyl ester in vitamin A-deficient rats. (A) Skeletal formulae of α-retinol and retinol and the chromatography internal standard β-*apo*-carotenol. (B) Representative absorbance spectra of the molecules shown in A. (C) Schematic of the experimental design. Vitamin A-deficient rats were dosed with 3.5 μmol (1 mg) of α-retinyl acetate; the livers, kidneys, and sera were harvested at 11 time points up to 336 h post-dose. The rats received no dose at the 0 h time point. (D) Representative chromatogram confirming detection of vitamin A forms in the rat serum at 7 h post-dose; liver and kidney chromatograms are shown in Figure S2A. (E) Time course plots showing changes in the retinol, α-retinol, and α-retinyl ester concentrations in the serum, liver, and kidney. Data are shown as means ± SEM; *P* values were calculated using the omnibus *F* test within a one-way ANOVA ($n = 5$ per time point).

pMF (pooled within each larynx); TA; and hAC. Liver tissue ($n = 5$) was obtained from the primary cadaver cohort. The samples (40–80 mg) were processed for protein isolation using a Qproteome Mammalian Protein Prep Kit (Qiagen) according to the manufacturer's instructions. Homogenization in lysis buffer was performed using a rotor-stator unit (TissueRuptor; Qiagen) for 30 s on ice followed by a probe ultrasonicator (300 V/T; Biologics) for 3 min (20 s on-off cycle) on ice. The protein concentration was measured using a DC Protein Assay (Bio-Rad) according to the manufacturer's instructions.

Protein isolates were incubated in Laemmli sample buffer containing 2-mercaptoethanol (Bio-Rad) at 95 °C for 5 min. Polyacrylamide gel electrophoresis was performed using 4–15% precast gels (mini-PROTEAN TGX, Bio-Rad) with 10 μg of total protein load per lane. Following transfer, polyvinylidene fluoride membranes were cut at 25 kDa and treated individually with 5% non-fat dry milk in Tris-buffered saline containing 0.05% Tween 20 at RT for 1 h, then incubated with primary antibodies at 4 °C overnight. Blots were detected using relevant HRP-conjugated secondary antibodies and enhanced chemiluminescence substrate (Pierce) at RT for 1 h. Imaging was performed using a BioSpectrum 815 system (Ultraviolet Products). To allow re-probing, primary and secondary antibodies were stripped from the membranes using Restore PLUS stripping buffer (Pierce) according to the manufacturer's instructions. Densitometric analysis was performed using ImageJ [19]; the band densities for each VF subsite were normalized to liver.

The primary antibodies used were rabbit anti-RBP1 (1:200; sc-30106, Santa Cruz), rabbit anti-STRA6 (1:500; H00064220-D01P, Novus), mouse anti-LPL (1:500, MABS1350, EMD Millipore), mouse anti-GFAP (1:200; G3893, Sigma–Aldrich), and rabbit anti-GAPDH (1:10000; ab181602, Abcam). The secondary antibodies used were HRP-conjugated goat anti-mouse and goat anti-rabbit IgG (1:5000; 31430 and 31460, Thermo Fisher).

2.9. Statistics

The total vitamin A concentration was defined as the sum of all of the (β form) retinol and retinyl ester concentrations; the total α-vitamin A concentration was defined as the sum of all of the α-retinol and α-retinyl ester concentrations. Esterification was calculated by dividing the retinyl ester (or α-retinyl ester) concentration by the total vitamin A (or total α-vitamin A) concentration and converting to a percentage. Thresholds for vitamin A deficiency and hypervitaminosis A were defined as 0.1 and 1.0 μmol/g total liver vitamin A, respectively, based on recent guidelines [20].

Data intended for statistical testing were first evaluated for normality and equality of variance using visual inspection of raw data plots, Levene's test, and the folded *F* test. Human vitamin A data were analyzed using analysis of covariance (ANCOVA), with the VFM concentration as the dependent variable; age, sex, body mass index, serum concentration, and liver concentration were used as covariates. Additional relationships between VFM, serum, and liver concentrations were analyzed using Pearson's *r*. Western blotting densitometric data were analyzed using one-way analysis of variance (ANOVA). Rat vitamin A data were analyzed using a *t* test in cases of two experimental groups or one-way ANOVA in cases of more than two experimental groups. All of the data analyzed using ANCOVA and ANOVA met normality and equality of variance assumptions; where indicated by the data, *t* tests were conducted under an unequal variance assumption (the Satterthwaite method). In all of the ANOVA models, if the *F* test revealed a significant difference, planned pairwise comparisons were performed using Fisher's protected least significant difference method. A type I error rate of 0.01 was used for all of the statistical testing; all of the *P* values were two-sided.

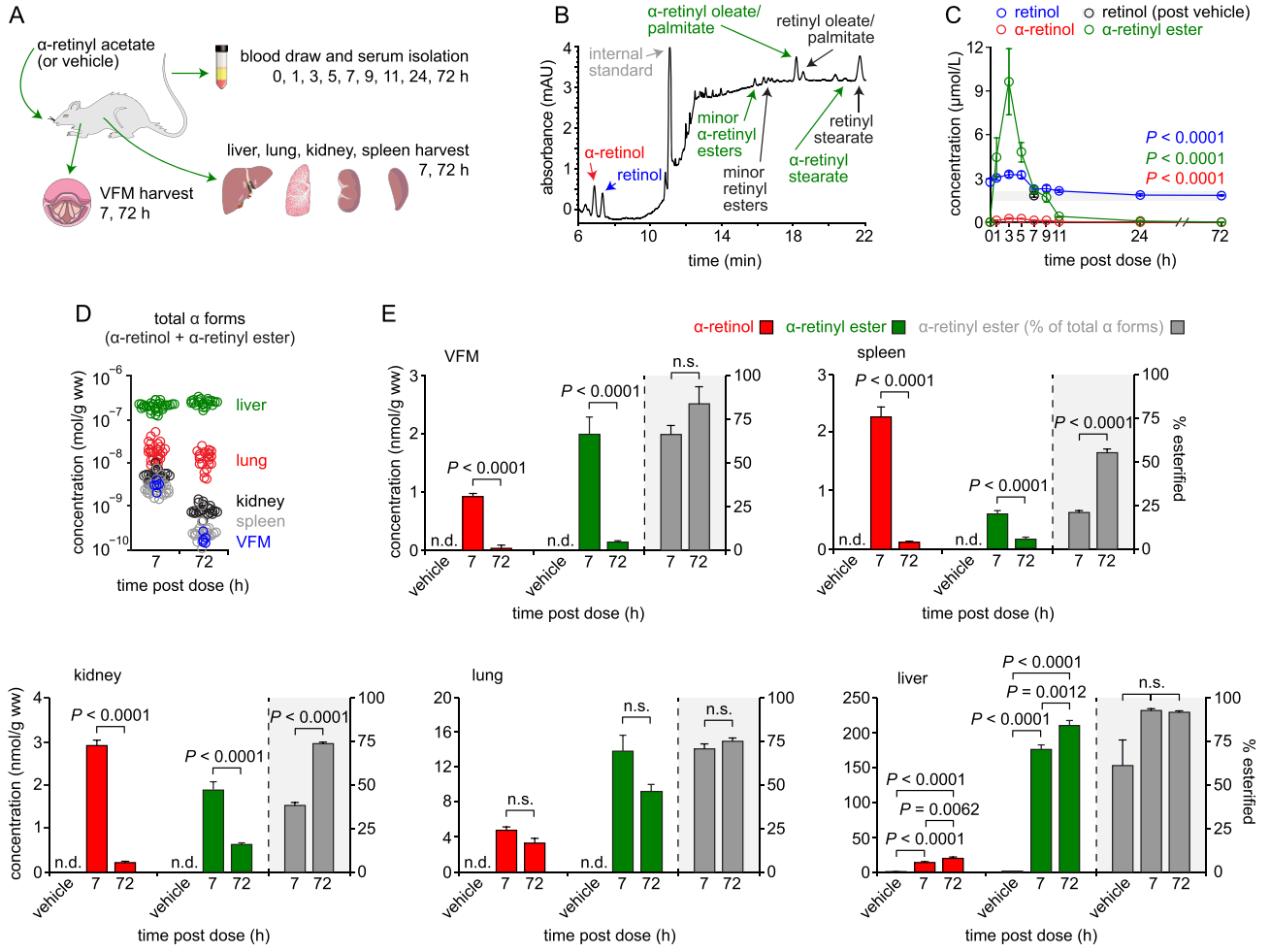

Figure 4: Uptake and utilization of α-retinyl ester in VFM compared to liver and other extrahepatic tissues in vitamin A-sufficient rats. (A) Schematic of the experimental design. Vitamin A-sufficient rats were dosed with 7 μmol (2 mg) of α-retinyl acetate; tissue and sera were collected at time points up to 72 h post-dose. The rats received no dose at the 0 h time point. (B) Representative chromatogram confirming the detection of vitamin A forms in the rat VFM at 7 h post-dose. The drift in baseline absorbance reflects a solvent transition during the gradient. (C) Time course plot showing retinol, α-retinol, and α-retinyl ester concentrations in the serum. Data are shown as means ± SEM; *P* values were calculated using the omnibus *F* test within a one-way ANOVA ($n = 5$–6 per time point). (D) Total α-vitamin A concentrations in all of the tissues at 7 and 72 h post-dose. (E) The α-retinol and α-retinyl ester concentrations and percent esterified α-vitamin A in all of the tissues at 7 and 72 h post-dose. Data are shown as means ± SEM; *P* values were calculated using a *t* test or one-way ANOVA ($n = 5$, pooled from 25 [VFM, 7 and 72 h]; $n = 25$–30 [other tissues, 7 and 72 h]; and $n = 5$ [other tissues, vehicle]). The VFM vehicle data were obtained from a single replicate pooled from 5 independent samples and not subjected to statistical analysis; n.d., not detected; n.s., non-significant difference.

3. RESULTS

3.1. Vitamin A storage in human VFM

The current understanding of vitamin A storage in human VFM is limited to intracellular staining of VF stellate cells with gold chloride [10,11], detection of vitamin A autofluorescence [10], and a single report on retinol and retinyl ester concentrations in three donors [11]. Despite its importance to VF biology, it is unknown how vitamin A storage in VFM corresponds to that of circulating plasma or liver, where most body reserves are housed [3]. To obtain baseline data, we procured VFM, liver, and serum from 26 human cadavers (Figure 1A) and assayed vitamin A forms and concentrations using UPLC. We used cadaveric donors because elective VFM biopsy risks iatrogenic damage in healthy individuals and analysis of liver tissue is the gold standard for assessing vitamin A status. The samples were obtained <16 h postmortem; the donors were mid- to late-life adult males ($n = 12$) and females ($n = 14$) with a broad range of body mass indices (Figure 1B). Rather than isolating the MF, we analyzed intact bilateral VFM pairs (with retention of aMF and pMF) to ensure that we captured all of the vitamin A-associated cells and allow comparison with prior data from humans and other species [11].

The donors exhibited a wide range of total liver vitamin A reserves (0.001–3.38 μmol/g; Figure 1C); the total vitamin A concentrations in the VFM (0.086–0.821 nmol/g) and serum (0.065–3.15 μmol/L) were more tightly clustered across individuals. Based on recent guidelines [20], 12 donors were classified as vitamin A sufficient (0.1–1.0 μmol/g liver), 6 were vitamin A deficient (<0.1 μmol/g liver), and 8 were hypervitaminotic (>1.0 μmol/g liver). The mean concentration in the VFM was 0.06% of that in the liver (0.416 ± 0.218 nmol/g vs 0.743 ± 0.971 μmol/g [mean ± SD], respectively) and higher than in previously reported data collected usingHPLC [11]. Liver vitamin A was primarily detected as retinyl esters (consistent with cytoplasmic

storage in hepatic stellate cells) [3], serum vitamin A was primarily detected as retinol (consistent with RBP4-mediated transport) [1], and VFM vitamin A was variably esterified (0—70.9%; Figure 1C).

We used ANCOVA to build a statistical model of the total vitamin A concentration in the VFM (omnibus $P = 0.0010$; Figure 1D). The serum concentration was the only significant predictor of the VFM concentration ($P = 0.0008$); the donor age, sex, body mass index, and liver concentrations were non-significant variables ($P = 0.017$—0.907). Regression analyses of the retinol and retinyl ester concentrations showed the strongest linear relationships between VFM and serum retinol ($r = 0.763$; $P < 0.0001$) and VFM and liver retinyl esters ($r = 0.726$; $P < 0.0001$). These findings are consistent with a physiologic relationship between vitamin A uptake and utilization in VFM with that available from circulating plasma and liver reserves.

To corroborate our UPLC data, we immunoassayed human VF for stellate cell, vitamin A uptake, and vitamin A utilization markers (Figure 2 and Fig. S1). The stellate cell marker glial fibrillary acidic protein (GFAP) [21,22] was predominantly expressed by cells in the aMF and pMF [11,23]; posteriorly, it exhibited a gradient of reduced immunosignal as the pMF transitioned into the eAC and then hAC. Stimulated by retinoic acid 6 (STRA6), the RBP4 cell-surface receptor and retinol transmembrane transporter [24] was strongly expressed by stellate cells, fibroblasts, and epithelial cells; in contrast, cellular retinol-binding protein 1 (RBP1), which accepts retinol from STRA6 and donates it as a substrate for esterification or oxidation [1,25], was weakly expressed. Lipoprotein lipase (LPL), a multifunctional enzyme that facilitates hydrolysis and cellular uptake of retinyl esters from chylomicra [26,27], was consistently expressed across the VF regions and cell types. Retinoic acid receptor-α (RARA) was expressed by stellate cells in the aMF and pMF, chondrocytes in the hAC, and luminal epithelial cells. In sum, these data confirm that human VFM contains distinct cell populations with the machinery to uptake, process, and metabolize retinol and retinyl esters from circulation.

3.2. Pharmacokinetics of single dose α-retinyl ester in vitamin A-deficient rats

To support our human characterization work with physiologic data, we used an *in vivo* rat model to assess vitamin A transport and pharmacokinetics. As vitamin A trafficking to VFM might involve both RBP4-dependent and -independent mechanisms, we used an α-retinyl ester dosing paradigm to test whether VFM can receive postprandial retinyl esters directly from chylomicra independent of RBP4. This approach takes advantage of the inability of α-retinol (distinguished from retinol [also known as β-retinol] by a shift of the cyclohexene ring double bond from the 5,6 to the 4,5 position; Figure 3A,B) to bind to RBP4 [28], meaning that while it can accumulate in the liver, it remains sequestered and cannot reenter the circulation for RBP4-mediated transport to extrahepatic organs [7,29]. Therefore, detection of α-vitamin A in extrahepatic tissue provides evidence of postprandial trafficking by chylomicra.

Before assaying VFM uptake, we piloted the approach in serum, liver, and kidneys after dosing vitamin A-deficient Sprague Dawley rats with a single 1 mg (3.5 μmol) α-retinyl acetate bolus (Figure 3C). We selected the rat strain and deficiency model based on precedence in the vitamin A literature [18,30,31] and because we reasoned that initial detection of α forms would be more straightforward in animals with reduced total body vitamin A; we selected the α-retinyl acetate dose based on prior research showing no liver toxicity at 3.5 μmol even after repeated administration [18]. Using HPLC, we detected α-vitamin A in all of the non-baseline samples up to 336 h post-dose (Figure 3D,E; Fig. S2A). Most of the dose detected in the serum was in α-retinyl ester form: the concentration peaked at 1.5 h and returned to baseline by 12 h. Liver uptake of α-retinyl esters (and, at lower concentrations, α-retinol) peaked at 24 h post-dose and then slowly declined, suggesting gradual hepatic utilization or release via a non-RBP4 mechanism. Kidney uptake was comparable for α-retinol and α-retinyl esters, with both concentrations peaking at 8 h post-dose. Finally, retinol and retinyl ester concentrations in the serum and liver varied across the monitoring period (Figure 3E and Fig. S2B), suggesting that, at least in the vitamin A-deficient condition, a single α-retinyl ester dose might impact the utilization of existing vitamin A stores.

3.3. Uptake and utilization of α-retinyl esters in vitamin A-sufficient rat VFM

Having successfully profiled the uptake and utilization of orally dosed α-retinyl ester in the serum, liver, and kidneys, we next evaluated single-dose pharmacokinetics in VFM (Figure 4A). We used Fischer 344 strain rats to allow comparison with prior VFM data [11]; we kept the rats in vitamin A-sufficient status to better evaluate the impact of postprandial α-vitamin A delivery on utilization of existing vitamin A stores. We added a vehicle control, expanded the extrahepatic comparison tissues to include the lungs and spleen, and narrowed the monitoring period to 72 h post-dose. Finally, as rat VFM is a relatively small tissue (>0.2 mm^3 [32,33]; ~0.8 g ww in our dataset) with stellate cells restricted to the aMF and pMF, we optimized detection and quantification by doubling the α-retinyl acetate dose to 2 mg (7 μmol), using UPLC in place of HPLC, and pooling bilateral VFM from 5 larynges per biological replicate. Preliminary analysis confirmed the detection of all of the α forms of interest (Figure 4B).

The serum α-retinyl ester concentration peaked at 3 h, approached baseline by 11 h, and was completely cleared from the circulation by 24 h post-dose (Figure 4C). We noted parallel but smaller spikes in the serum retinol and α-retinol concentrations, presumably due to the dose overwhelming the enterocyte esterification apparatus, leading to co-packaging of intestinal retinol and α-retinol with α-retinyl esters in chylomicra. The total α-vitamin A concentrations at 7 and 72 h were highest in the liver, followed by the lungs, kidneys, spleen, and VFM (Figure 4D); the concentrations in all of the extrahepatic tissues decreased between 7 and 72 h. VFM α-retinol and α-retinyl esters (0.931 ± 0.048 and 2.00 ± 0.284 nmol/g at 7 h, respectively) were nearly completely metabolized by 72 h (Figure 4E). The spleen and kidneys showed the most similar concentration profiles to that of VFM with the exception that the initial uptake (7 h) in both tissues favored α-retinol over α-retinyl esters. In contrast to these fast-metabolizing tissues, the lungs retained the majority of absorbed α-vitamin A and the liver accumulated additional α-vitamin A through 72 h post-dose. Finally, we observed extrahepatic retinol uptake (VFM, kidneys, and lungs) and utilization (spleen and kidneys) at 7 and 72 h (Fig. S3), consistent with these tissues absorbing the α-retinyl ester dose alongside chylomicron-co-packaged or RBP4-bound retinol from the circulation.

3.4. Characterization of stellate cell- and vitamin A-associated markers in vitamin A-sufficient rat VF

We immunostained vitamin A-sufficient rat VF for stellate cell and vitamin A uptake, storage, and utilization markers. Consistent with human VF (Figure 2 and Fig. S1), GFAP was expressed by stellate cells in the aMF and pMF as well as chondrocytes in the eAC (Figure 5A). Most of the $GFAP^+$ VF stellate cells (and neighboring $GFAP^+$ eAC cells) strongly co-expressed STRA6 and RARA; a subset was $GFAP^+LPL^+$ (Figure 5B). As vitamin A reserves are stored as retinyl esters within cytoplasmic lipid droplets [1], we additionally probed tissues with lipophilic dye boron-dipyrromethene (BODIPY) and assessed the

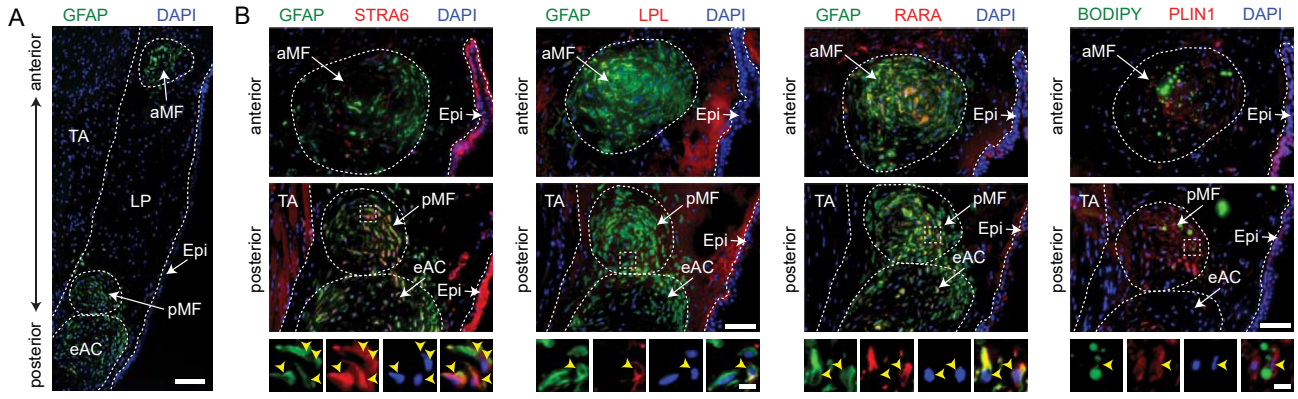

Figure 5: Characterization of stellate cell- and vitamin A-associated markers in vitamin A-sufficient rat VF. (A) Representative axial section immunostained for GFAP. The white dashed lines indicate the aMF, pMF, eAC, and boundaries between the TA, LP, and Epi. Scale bar, 100 μm. (B) Additional axial sections showing colocalization of GFAP with STRA6, LPL, and RARA, as well as BODIPY with PLIN1, within the aMF and pMF. The white dashed boxes indicate pMF regions that are enlarged (below) as high-magnification, single- and merged-channel images. The yellow arrowheads indicate $GFAP^{+}STRA6^{+}$, $GFAP^{+}LPL^{+}$, $GFAP^{+}RARA^{+}$, and $BODIPY^{+}PLIN^{+}$ stellate cells. Scale bar, 50 μm (low-magnification images) and 10 μm (high-magnification images).

distribution of lipid droplet coating protein perilipin 1 (PLIN1). Most of the VF stellate cells were $PLIN^{+}$; a subset was $BODIPY^{+}$. Assessment of additional VF regions showed STRA6 and RARA expression patterns (Figs. S4 and S5) that were comparable to those observed in human tissue (Fig. S1); LPL was weakly expressed in the TA and by a small subset of epithelial cells (Fig. S6); BODIPY was detected in the hAC and PLIN1 was weakly expressed by basal epithelial cells (Fig. S7). Overall, these immunostaining data corroborate our α-retinyl ester dosing results by confirming that, as in humans, rat VFM cells have the requisite machinery to uptake, process, store, and metabolize vitamin A irrespective of the (RBP4-dependent or -independent) delivery mechanism.

4. DISCUSSION

Using human cadavers and an *in vivo* rat system, we herein provide the first physiologic analysis of vitamin A uptake, storage, and utilization within VFM benchmarked to liver, serum, and other extrahepatic tissues. Our data confirm VFM as a *bona fide* extrahepatic vitamin A repository in the larynx, advance characterization of the VF stellate cell phenotype, and show general biologic concordance between humans and rats. Notably, approximately half ($n = 14$; 54%) of the humans in our cadaver cohort met the gold standard (total liver reserve) criteria for vitamin A deficiency or hypervitaminosis A [20]. While both conditions are assumed to exist in the US adult population [34], definitive liver biopsy-based assessment is rare in humans. The high prevalence estimates in our cohort may reflect inadequate micronutrient intake in certain individuals [35–37], overconsumption of fortified foods and supplements in others [38,39], and medical comorbidities and end-of-life interventions in some.

Analysis of the complete dataset allowed us to build a statistical model of vitamin A utilization based on a wide range of biologically and clinically relevant concentrations. Serum vitamin A was the only significant predictor of the VFM concentration in the full model, suggesting that VFM stores may be rapidly metabolized *in situ* and replenished from the circulatory pool. Further, VFM vitamin A favored the retinol form but exhibited a range of esterification across individuals, consistent with the dynamic management of metabolic and storage needs. We corroborated these observations using immunodetection of vitamin A-associated markers and pharmacokinetic profiling of orally dosed α-retinyl ester in rats. Prior research showed that α-retinol has 40–50% of the biopotency of retinol [18]; in VFM, these molecules presumably support the same biologic functions. On a vitamin A-sufficient background, dosed α-vitamin A was detected in rat VFM in both ester and alcohol forms, indicating postprandial trafficking by chylomicra and initial hydrolysis followed by some esterification. Both α forms were nearly fully depleted by 72 h, confirming the high metabolic demand for vitamin A within VFM.

It is well-established that VFM vitamin A is stored locally by stellate cells in the aMF and pMF [10,11]. Our observation of cytoplasmic RARA in human and rat VF stellate cells was consistent with a prior report [12] and suggests that these vitamin A-storing cells may additionally metabolize retinoic acid. Importantly, while classically known as a nuclear receptor and transcription factor, RARA can localize to the cytoplasm in quiescent cells and undergo nuclear translocation when retinoic acid is present [40,41]. In fact, RARs appear to mediate the pleiotropic functions of retinoids in part by operating in multiple subcellular compartments [42–45]. The VF stellate cell phenotype is distinct from that of VF epithelial cells, which preferentially express nuclear RARB [13], do not retain retinyl esters for storage [11], and are highly sensitive to vitamin A bioavailability [13,14]. While our data further show that VF epithelial cells strongly and uniformly express STRA6, it is unclear whether vitamin A is supplied to the VF epithelium by neighboring stellate cells or the circulatory pool.

By demonstrating uptake of dosed α-vitamin A from chylomicra, we show that, in addition to plasma retinol and the local VF stellate cell repository, VFM can directly access postprandial retinyl esters to meet metabolic demands. The total VFM uptake under vitamin A-sufficient conditions presumably involves a combination of RBP4-dependent and -independent transport: future research could quantify the relative dependence on each mechanism by comparing α-retinyl ester kinetics with that of a retinoid tracer capable of binding RBP4 (for example, 3,4-didehydroretinyl ester [also known as vitamin A_2]) [8,9,18]. Future research should also examine whether subpopulations of VFM cells uptake vitamin A via the same or different mechanisms, if they do so in a coordinated or independent fashion, and whether they use established or novel metabolic pathways for intracellular vitamin A processing.

AUTHOR CONTRIBUTIONS

N.V.W. and S.A.T. conceived and designed this study. K.N. and Y.T. coordinated cadaver sample procurement and conducted all of the

microdissections. C.R.D. performed HPLC of human tissue and serum. S.A.T. synthesized the α-retinyl acetate. K.N. and C.R.D. conducted the primary α-retinyl acetate experiment and C.R.D. performed UPLC. K.N. performed all of the histology, immunodetection assays, and microscopy. K.N. and N.V.W. analyzed the data and wrote the manuscript. All of authors reviewed and approved the final version.

ACKNOWLEDGMENTS

We thank Erin Brooks and Jodi Corbit for tissue procurement and Glen Leverson and Lily Stalter for statistical consultation. This study was supported by grants R01 DC004428 and R01 DC010777 from the National Institute on Deafness and Other Communication Disorders and grant 2007-35200-17729 from the US Department of Agriculture Research Initiative.

CONFLICT OF INTEREST

None declared.

APPENDIX A. SUPPLEMENTARY DATA

Supplementary data to this article can be found online at https://doi.org/10.1016/j.molmet.2020.101025.

REFERENCES

[1] Blomhoff, R., Green, M.H., Berg, T., Norum, K.R., 1990. Transport and storage of vitamin A. Science 250(4979):399–404.

[2] D'Ambrosio, D.N., Clugston, R.D., Blaner, W.S., 2011. Vitamin A metabolism: an update. Nutrients 3(1):63–103.

[3] Friedman, S.L., 2008. Hepatic stellate cells: protean, multifunctional, and enigmatic cells of the liver. Physiological Reviews 88(1):125–172.

[4] Senoo, H., Mezaki, Y., Fujiwara, M., 2017. The stellate cell system (vitamin A-storing cell system). Anatomical Science International 92(4):387–455.

[5] Paik, J., Vogel, S., Quadro, L., Piantedosi, R., Gottesman, M.E., Lai, K., et al., 2004. Vitamin A: overlapping delivery pathways to tissues from the circulation. Journal of Nutrition 134(1):276S–280S.

[6] O'Byrne, S.M., Blaner, W.S., 2013. Retinol and retinyl esters: biochemistry and physiology. Journal of Lipid Research 54(7):1731–1743.

[7] Dever, J.T., Surles, R.L., Davis, C.R., Tanumihardjo, S.A., 2011. α-Retinol is distributed through serum retinol-binding protein-independent mechanisms in the lactating sow-nursing piglet dyad. Journal of Nutrition 141(1):42–47.

[8] Surles, R.L., Mills, J.P., Valentine, A.R., Tanumihardjo, S.A., 2007. One-time graded doses of vitamin A to weanling piglets enhance hepatic retinol but do not always prevent vitamin A deficiency. American Journal of Clinical Nutrition 86(4):1045–1053.

[9] Sun, T., Surles, R.L., Tanumihardjo, S.A., 2008. Vitamin A concentrations in piglet extrahepatic tissues respond differently ten days after vitamin A treatment. Journal of Nutrition 138(6):1101–1106.

[10] Sato, K., Hirano, M., Nakashima, T., 2003. Vitamin A-storing stellate cells in the human vocal fold. Acta Oto-Laryngologica 123(1):106–110.

[11] Toya, Y., Riabroy, N., Davis, C.R., Kishimoto, Y., Tanumihardjo, S.A., Bless, D.M., et al., 2014. Interspecies comparison of stellate cell-containing macula flava and vitamin A storage in vocal fold mucosa. Journal of Anatomy 225(3):298–305.

[12] Tateya, T., Tateya, I., Surles, R.L., Tanumihardjo, S.A., Bless, D.M., 2008. Roles of vitamin A and macula flava in maintaining vocal folds. Annals of Otology, Rhinology and Laryngology 117(1):65–73.

[13] Tateya, I., Tateya, T., Surles, R.L., Kanehira, K., Tanumihardjo, S.A., Bless, D.M., 2008. Vitamin A deficiency causes metaplasia in vocal fold epithelium: a rat study. Annals of Otology, Rhinology and Laryngology 117(2):153–158.

[14] Tateya, I., Tateya, T., Surles, R.L., Tanumihardjo, S.A., Bless, D.M., 2007. Prenatal vitamin A deficiency causes laryngeal malformation in rats. Annals of Otology, Rhinology & Laryngology 116(10):785–792.

[15] Issing, W.J., Struck, R., Naumann, A., 1996. Long-term follow-up of larynx leukoplakia under treatment with retinyl palmitate. Head & Neck 18(6):560–565.

[16] Olsen, K., Suri, D.J., Davis, C., Sheftel, J., Nishimoto, K., Yamaoka, Y., et al., 2018. Serum retinyl esters are positively correlated with analyzed total liver vitamin A reserves collected from US adults at time of death. American Journal of Clinical Nutrition 108(5):997–1005.

[17] Tanumihardjo, S.A., 2001. Synthesis of 10,11,14,15-$^{13}C_4$-and 14,15-$^{13}C_2$-retinyl acetate. Journal of Labelled Compounds and Radiopharmaceuticals 44(5):365–372.

[18] Riabroy, N., Dever, J.T., Tanumihardjo, S.A., 2014. α-Retinol and 3,4-didehydroretinol support growth in rats when fed at equimolar amounts and α-retinol is not toxic after repeated administration of large doses. British Journal of Nutrition 111(8):1373–1381.

[19] Schneider, C.A., Rasband, W.S., Eliceiri, K.W., 2012. NIH Image to ImageJ: 25 years of image analysis. Nature Methods 9(7):671–675.

[20] Tanumihardjo, S.A., Russell, R.M., Stephensen, C.B., Gannon, B.M., Craft, N.E., Haskell, M.J., et al., 2016. Biomarkers of nutrition for development (BOND)-vitamin A review. Journal of Nutrition 146(9):1816S–1848S.

[21] Niki, T., de Bleser, P.J., Xu, G., van den Berg, K., Wisse, E., Geerts, A., 1996. Comparison of glial fibrillary acidic protein and desmin staining in normal and CCl4-induced fibrotic rat livers. Hepatology 23(6):1538–1545.

[22] Xu, L., Hui, A.Y., Albanis, E., Arthur, M.J., O'Byrne, S.M., Blaner, W.S., et al., 2005. Human hepatic stellate cell lines, LX-1 and LX-2: new tools for analysis of hepatic fibrosis. Gut 54(1):142–151.

[23] Sato, K., Umeno, H., Nakashima, T., 2012. Vocal fold stellate cells in the human macula flava and the diffuse stellate cell system. Annals of Otology, Rhinology and Laryngology 121(1):51–56.

[24] Kawaguchi, R., Yu, J., Honda, J., Hu, J., Whitelegge, J., Ping, P., et al., 2007. A membrane receptor for retinol binding protein mediates cellular uptake of vitamin A. Science 315(5813):820–825.

[25] Uchio, K., Tuchweber, B., Manabe, N., Gabbiani, G., Rosenbaum, J., Desmoulière, A., 2002. Cellular retinol-binding protein-1 expression and modulation during in vivo and in vitro myofibroblastic differentiation of rat hepatic stellate cells and portal fibroblasts. Laboratory Investigation 82(5):619–628.

[26] Blaner, W.S., Obunike, J.C., Kurlandsky, S.B., Al-Haideri, M., Piantedosi, R., Deckelbaum, R.J., et al., 1994. Lipoprotein lipase hydrolysis of retinyl ester. Possible implications for retinoid uptake by cells. Journal of Biological Chemistry 269(24):16559–16565.

[27] van Bennekum, A.M., Kako, Y., Weinstock, P.H., Harrison, E.H., Deckelbaum, R.J., Goldberg, I.J., et al., 1999. Lipoprotein lipase expression level influences tissue clearance of chylomicron retinyl ester. Journal of Lipid Research 40(3):565–574.

[28] Muhilal, H., Glover, J., 1975. The affinity of retinol and its analogues for retinol-binding protein. Biochemical Society Transactions 3(5):744–746.

[29] Riabroy, N., Tanumihardjo, S.A., 2014. Oral doses of α-retinyl ester track chylomicron uptake and distribution of vitamin A in a male piglet model for newborn infants. Journal of Nutrition 144(8):1188–1195.

[30] Ross, A.C., Li, N.-Q., 2007. Lung retinyl ester is low in young adult rats fed a vitamin A deficient diet after weaning, despite neonatal vitamin A supplementation and maintenance of normal plasma retinol. Journal of Nutrition 137(10):2213–2218.

[31] Tanumihardjo, S.A., Olson, J.A., 1988. A modified relative dose-response assay employing 3,4-didehydroretinol (vitamin A_2) in rats. Journal of Nutrition 118(5):598–603.

[32] Kurita, S., Nagata, K., Hirano, M., 1983. A comparative study of the layer structure of the vocal fold. In: Bless, D.M., Abbs, J.H. (Eds.), Vocal fold physiology: contemporary research and clinical issues. San Diego, CA: College-Hill Press. p. 3–21.

[33] Ling, C., Yamashita, M., Waselchuk, E.A., Raasch, J.L., Bless, D.M., Welham, N.V., 2010. Alteration in cellular morphology, density and distribution in rat vocal fold mucosa following injury. Wound Repair and Regeneration 18(1):89–97.

[34] US Centers for Disease Control and Prevention, 2012. Second national report on biochemical indicators of diet and nutrition in the US population 2012. Atlanta, GA.

[35] Duitsman, P.K., Cook, L.R., Tanumihardjo, S.A., Olson, J.A., 1995. Vitamin A inadequacy in socioeconomically disadvantaged pregnant Iowan women as assessed by the modified relative dose-response (MRDR) test. Nutrition Research 15(9):1263–1276.

[36] Spannaus-Martin, D.J., Cook, L.R., Tanumihardjo, S.A., Duitsman, P.K., Olson, J.A., 1997. Vitamin A and vitamin E statuses of preschool children of socioeconomically disadvantaged families living in the midwestern United States. European Journal of Clinical Nutrition 51(12):864–869.

[37] Bailey, R.L., Pac, S.G., Fulgoni, V.L., Reidy, K.C., Catalano, P.M., 2019. Estimation of total usual dietary intakes of pregnant women in the United States. JAMA Network Open 2(6):e195967.

[38] Kantor, E.D., Rehm, C.D., Du, M., White, E., Giovannucci, E.L., 2016. Trends in dietary supplement use among US adults from 1999-2012. Journal of the American Medical Association 316(14):1464–1474.

[39] Valentine, A.R., Davis, C.R., Tanumihardjo, S.A., 2013. Vitamin A isotope dilution predicts liver stores in line with long-term vitamin A intake above the current Recommended Dietary Allowance for young adult women. American Journal of Clinical Nutrition 98(5):1192–1199.

[40] Fukunaka, K., Saito, T., Wataba, K., Ashihara, K., Ito, E., Kudo, R., 2001. Changes in expression and subcellular localization of nuclear retinoic acid receptors in human endometrial epithelium during the menstrual cycle. Molecular Human Reproduction 7(5):437–446.

[41] Park, U.-H., Kim, E.-J., Um, S.-J., 2010. A novel cytoplasmic adaptor for retinoic acid receptor (RAR) and thyroid receptor functions as a derepressor of RAR in the absence of retinoic acid. Journal of Biological Chemistry 285(44): 34269–34278.

[42] Katagiri, Y., Takeda, K., Yu, Z.X., Ferrans, V.J., Ozato, K., Guroff, G., 2000. Modulation of retinoid signalling through NGF-induced nuclear export of NGFI-B. Nature Cell Biology 2(7):435–440.

[43] Cao, X., Liu, W., Lin, F., Li, H., Kolluri, S.K., Lin, B., et al., 2004. Retinoid X receptor regulates Nur77/TR3-dependent apoptosis by modulating its nuclear export and mitochondrial targeting. Molecular and Cellular Biology 24(22): 9705–9725.

[44] Dey, N., De, P.K., Wang, M., Zhang, H., Dobrota, E.A., Robertson, K.A., et al., 2007. CSK controls retinoic acid receptor (RAR) signaling: a RAR-c-SRC signaling axis is required for neuritogenic differentiation. Molecular and Cellular Biology 27(11):4179–4197.

[45] Han, Y.-H., Zhou, H., Kim, J.-H., Yan, T.-D., Lee, K.-H., Wu, H., et al., 2009. A unique cytoplasmic localization of retinoic acid receptor-gamma and its regulations. Journal of Biological Chemistry 284(27):18503–18514.

